Compressed Sensing Image Reconstruction for CASA

Jonas Schwammberger

August 14, 2018

Abstract

Image reconstruction from under-sampled measurements is a problem existing in the fields of MRI scans and Radio Astronomy. Applying the Theory of compressed Sensing, one is able to reconstruct the observed image by including prior information. A proof of concept Compressed Sensing reconstruction algorithm was applied to radio astronomy and implemented in the Common Astronomy Software Applications (CASA). The Reconstruction was compared to the standard algorithm in Astronomy, CLEAN. It was shown that with Compressed Sensing, we can modify the prior as we make new discoveries about the universe.

Contents

1 Reconstruction from under-sampled Measurements

In Signal Processing, continuous signals are represented with discrete samples. A digital recording of music, an image of a tree, or the measured velocity of a particle, all are discrete samples of continuous signals. The Nyquist-Shannon sampling rate tells us how many samples are needed to fully represent a signal: A signal which contains at most frequency f should be sampled with a frequency higher than $2f$. If we record a piece of music where the highest tone is at 20kHz, sampling rate should be more than 40kHz. Then, the music piece gets recorded above the Nyquist-Shannon sampling rate. It is fully sampled and there is exactly one continuous signal(with maximum frequency f) which fits the measurement.

The Nyquist-Shannon sampling rate is not always achievable: Samples may be expensive to acquire, get lost, or incomplete by the nature of the measurement instrument. In this case we are dealing with under-sampled measurements. Many possible signals fit the measurement and from the measurement alone, we cannot distinguish the true signal from all possibilities.

With the Theory of Compressed Sensing[1][2] however, we can use prior information about the signal and find the most likely candidate from all possibilities. Under the right conditions, the most likely candidate is guaranteed to be the true signal. With the Theory of Compressed Sensing, we exploit prior information to reconstruct the true signal from under-sampled measurements.

In this project, the Theory of Compressed Sensing was applied to an image reconstruction problem of Radio Astronomy. Interferometers produce under-sampled measurements of the sky which have to be reconstructed by an algorithm. A Compressed Sensing approach was developed and implemented in the Common Astronomy Software Application (CASA). The reconstruction quality was compared to standard reconstruction algorithm in astronomy on VLA data of Supernova Remnant G55.

1.1 Image Reconstruction for Radio Interferometers

A Radio Interferometer consists of several antennas spaced apart from each other. Each antenna pair measures the different arrival time of a radio wave. For small field of view imaging, each antenna pair measures approximately a two dimensional Fourier components of the sky (called Visibility in Astronomy). An interferometer with 26 antennas measures 325 Visibilities. The distance between the antenna pair(called a baseline) dictates which Visibility of the image gets observed. The longer the baseline, the higher frequency of the observed Visibility. The longest baseline of an interferometer is therefore a rough estimate of its maximum resolution.

For wide field of view imaging, the two dimensional Fourier relation breaks apart as additional effects dominate the measurement. This project uses small field of view imaging, and the two dimensional Fourier component is a good approximation. In this document, a measured Visibility is used as a synonym for two dimensional Fourier component.

The interferometer only samples as many Visibilities as it has antenna pairs. In general, we do not have all Visibilities needed to reconstruct the image. The task is therefore to reconstruct the observed image from an under-sampled Fourier space. In Astronomy, the CLEAN class of algorithms[3][4][5][6] were developed for this task. New interferometers like MeerKAT also observe new phenomenons which, in an ideal world, can be included in the CLEAN prior and improve its reconstruction. This is not possible in CLEAN, the prior is a fixed part of the algorithm. It cannot be modified as our prior knowledge of radio images increases.

Compressed Sensing can be thought of as a generalization of the CLEAN algorithm. The prior can be exchanged without changing the rest of the reconstruction algorithm. Furthermore experiments suggest Compressed Sensing reconstructions may be able to super-resolve the image[7].

1.2 Deconvolution of the Dirty Image

A real world interferometer corrupts the observed image with the image with under-sampling and other instrumental effects. The inverse Fourier Transform of the Visibilities can still be calculated, but it results in a corrupted ”dirty” image. The observed image is convolved with a Point Spread Function (PSF). The task is to reconstruct the observed image from the dirty image and the PSF, or more formally we try to solve for x in equation (1.1), where only the PSF and I_{dirty} are known($\star$ is used as the convolution operation).

$$x \star PSF + N = I_{dirty} \tag{1.1}$$

A deconvolution algorithm should find the observed image x. However, there may be many possible solutions to the equation (1.1). Noise N further complicates the deconvolution. The algorithm has to decide what is the most likely x given PSF and I_{dirty}. The PSF is specific to the interferometer. It models the sampling pattern in Fourier space. A deconvolution algorithm is not limited to a single interferometer and can easily be used on other instruments[1].

Note that the deconvolution problem is just one way of formulating the reconstruction. It was used in this project since the CASA interface was built for deconvolution algorithms. The same problem can be formulated as in-painting the missing Visibilities: If we apply the Fourier Transform to equation (1.1), then the convolution turns to a multiplication and we arrive at a similar equation $X * M + N = V$. The Fourier Transform of I_{dirty} is just the measured Visibilities V, PSF turns into a masking matrix M. M is one for all measured Visibilities and zero everywhere else. If an algorithm can in-paint the missing Visibilities X, it has also found a solution x to the deconvolution problem of (1.1). In section 2.2 the different formulations get discussed in more detail.

1.3 Deconvolution with CLEAN

CLEAN assumes the image consists of single pixel wide point sources. This is true when the image contains stars, the majority of which are too far away from earth to have any extension. CLEAN therefore takes a dirty image and a PSF as input and tries to find point sources in the image. In each iteration of CLEAN, it searches the highest peak of the dirty image. It removes a fraction of the PSF at the maximum and adds the peak into a separate ”model” image. Over many iterations, it fills the model image with ”cleaned” peaks. It stops until the next highest peak is below a threshold, or if the maximum number of iterations was reached. The fraction of the PSF, threshold and number of iterations are tunable by the user.

CLEAN optimizes the objective (1.2) which is split in a data and a regularization term. The data term forces CLEAN to reconstruct close to the measurements, while the regularization term should account for noise. In each iteration, CLEAN searches the step which minimizes the objective the most, it uses a greedy optimization scheme. Due to the L0 ”norm”[2], the objective is non-convex and it may have local minima. Note that the L0 ”norm” acts as the sum of non-zero elements in the image.

$$\underset{x}{minimize} \ \|I_{dirty} - x \star PSF\|_2^2 + \ \|x\|_0 \tag{1.2}$$

In practice, CLEAN gets stopped before it reaches a local minima. A common stopping criteria is if the next peak in the dirty image is below 3 to 5 times the estimated noise level. In that case, CLEAN detects all peaks that are higher than 3 to 5 times the estimated noise.

[1] This is true for small field of view imaging. Wide field of view introduces additional effects that typically do not get modelled with a PSF.

[2] The L0 ”norm” in this context is technically not a norm, hence the quotation marks. The L0 ”norm” is a common notation in Compressed Sensing literature, therefore it is used here.

CLEAN does a good approximation of the observed image, if it contains only point sources. Radio images may also contain extended emissions like hydrogen clouds, which are spread over several pixels. The maximum brightness of extended emissions tends to be lower than point sources and CLEAN is prone to ignore extended emission. Even if the emission is above the threshold, CLEAN approximates extended emissions with faint point sources. Instead of a hydrogen clouds, CLEAN may detect a cluster of faint stars.

To combat the problem, the reconstructed image of CLEAN gets convolved with the antenna beam-pattern. The beam-pattern is approximately a two dimensional Gaussian and represents the accuracy of the antennas. Clusters of faint stars get blurred into a more plausible cloud. This essentially lowers the resolution of the reconstructed image. The rationale is that any higher resolved structure is likely a reconstruction artefact. Over the years, the algorithm was extended, with the MS-MFS-CLEAN[6] as a recent example. All versions do blur the reconstructed image with the antenna beam-pattern.

The CLEAN prior works well for point sources, but it does not accurately reconstruct extended emissions. With the right prior super-resolved image reconstruction is possible. It was demonstrated in laboratory environment with the One Pixel Camera[8], or with the SASIR[7] reconstruction algorithm for the LOFAR radio interferometer. Since the prior of CLEAN is a fixed part of the algorithm it cannot be modified without creating a new algorithm.

1.4 CLEAN as Compressed Sensing Image Reconstruction

Compressed Sensing Image Reconstruction is a generalization of the CLEAN algorithm. A Compressed Sensing Reconstruction algorithm consists of three separate parts:

- An objective with a data and regularization term, and a parameter λ.
- A prior function $p()$.
- An optimization algorithm.

As the prior function $p()$, CLEAN uses the L0 ”norm”. The optimization algorithm is similar to Matching Pursuit. In each iteration, Matching Pursuit searches the element in the regularization term that minimizes the objective the most. The objective of CLEAN can also be generalized into (1.3). The objective still has a data and regularization term, but now the parameter λ represents the trade-off between reconstructing close to the measurement and reconstructing a plausible image.

$$\underset{x}{minimize} \ \|I_{dirty} - x \star PSF\|_2^2 \ + \ \lambda \, p(x) \tag{1.3}$$

CLEAN is similar to a Compressed Sensing Reconstruction consisting of the L0 ”norm”, matching pursuit and the objective (1.3). But now, individual parts of the Compressed Sensing Reconstruction can be replaced. For example instead of the L0 ”norm”, one could use the L2 norm, or apply the Haar Transform and use the L0 ”norm” on the Haar Wavelet coefficients of x. The prior function $p()$ can be chosen according to our prior knowledge and potentially super-resolve the image x.

2 Compressed Sensing Image Reconstruction

We want to reconstruct an image from under-sampled measurements. We can retrieve the true image if:

- we have prior information about the image
- measurement space and reconstruction space are incoherent

Let us assume there are s point sources in the image and we use the L0 ”norm” as the regularization. If we would know the number and location of the s point sources, we could sample the s pixels to determine their magnitude. Sadly, we do not know the location before in general. The naive approach is therefore to sample at every pixel location. However, this is wasteful: Note that if we land at an empty pixel, the sample gives us almost no new information. If we would sample the whole image pixel for pixel, our average information gain per sample is low. In the under-sampled environment, we only have a limited number of samples available, we want to maximize the information gained for each sample. This is the case when the measurement space is incoherent from the reconstruction space.

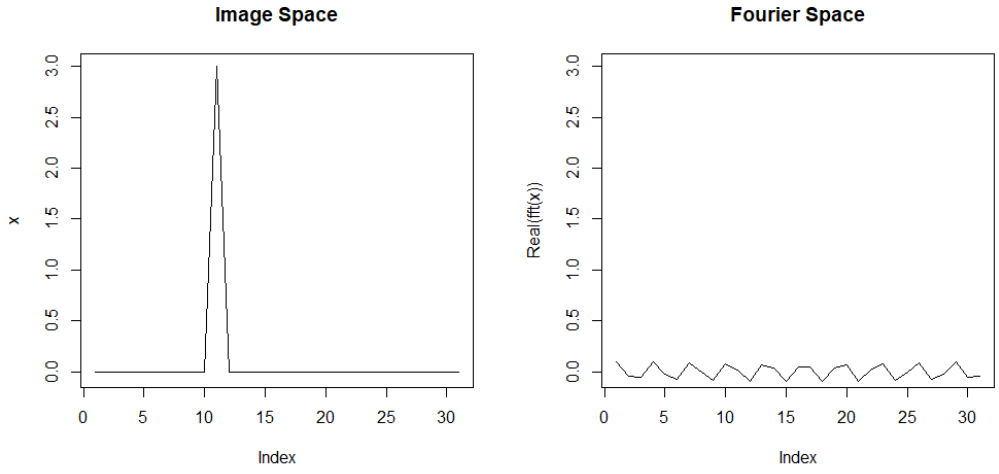

Figure 1: Image space and Fourier Space are maximally incoherent.

Interferometers measure in the Fourier domain, which is maximally incoherent from the image domain. Figure 1 shows the change in the Fourier Space, when a single pixel is changed. A change in a single pixel will result in a small change for all Visibilities, while a change in a single Visibility will modify all pixels. Intuitively, with each Visibility we now learn information about the s point sources. The average information gain per sample is maximized and we can reconstruct the even from under-sampled measurements. It works because we only need information about the s non-zero pixels.

The question remains, how many samples are needed to reconstruct the image? The answer to that question is an active field of research[9], but depends (among other factors) on the number of non-zero entries s in the prior. If the image also contains extended emissions, it increases the number of non-zero pixels s, which in turn increases the needed samples. However, if we can represent the image in a more sparse domain, we can reconstruct the image from fewer samples.

2.1 Sparseland Prior and over-complete Representations

An image containing both point sources and extended emissions is not sparse in the image domain. When using the L0 ”norm” as the prior, we want to reconstruct in a domain where the image can be as sparsely

represented as possible. From image compression, we know that natural images tend to be sparse in the Wavelet domain. We can use for example the Haar transform in the prior: $p(x) = \|Hx\|_0$ and potentially have a more sparse representation.

But why limit the prior to Wavelets? The prior function can be designed as we wish. Wavelets, sine functions or splines together can be used for the reconstruction. In practice many Compressed Sensing applications use a "sparseland" prior (2.1), a matrix D where each column contains a potential part of the image. The dictionary matrix D is potentially a large, but has a finite number entries. Any image x we measure consists only of a few entries of D. This means the coefficients for the signal parts in the dictionary α are all zero except for s entries for all valid x.

$$\begin{aligned} x = D\alpha \qquad x \in \mathbb{R}^n, \alpha \in \mathbb{R}^m, D \in \mathbb{R}^{n*m}, \qquad n \leq m \\ \|\alpha\|_0 = s \qquad s \ll n \leq m \end{aligned} \tag{2.1}$$

D can be a mixture of different functions that together model our image. We know point sources are sparse in the image domain, we can use the identity matrix (also sometimes called Dirac basis), which represents single pixel values, and further add columns consisting of wavelets. The number of columns m can be much larger than the number of pixels n, which lends itself to over-complete representations.

An over-complete dictionary has more columns than rows (more entries in the dictionary than pixels) and can be used represent an image with even fewer non-zero entries s. Starlets[10] and Curvelets[11] have been developed as over-complete representations for astronomy. In theory, there is no limitation on how many columns we add, but in practice computational power limits the size of D.

Sparseland priors are used with either the L0 "norm" or the L1 norm. The L0 "norm" pushes the objective into non-convex territory. There are specialized optimizers for L0 objectives that approximate the optimum well enough for practical applications. The L0 norm can be relaxed to L1, which results in a convex objective and is practically guaranteed to have the same optimum. In this project, the Gurobi[12] optimizer was used with the L1 relaxation.

2.2 Choosing the Objective Function

In general, there are three different reconstruction objectives: The analysis method, where the image x is minimized directly, the synthesis method where the sparse vector α is minimized, or by in-painting the missing Visibilities V_2.

$$\begin{aligned} analysis: \qquad & \underset{x}{minimize} \ \|I_{dirty} - x \star PSF\|_2^2 \quad + \lambda \left\|D^{-1}x\right\|_1 \\ synthesis: \qquad & \underset{\alpha}{minimize} \ \|I_{dirty} - D\alpha \star PSF\|_2^2 + \lambda \|\alpha\|_1 \\ in-painting: \qquad & \underset{V_2}{minimize} \ \left\|I_{dirty} - F^{-1}MV_2\right\|_2^2 \ + \lambda \left\|D^{-1}F^{-1}V_2\right\|_1 \end{aligned}$$

All three objective functions have the same global minimum. Retrieving x for the analysis objective is trivial. For the second and third objective x can be retrieved by $x = D\alpha$ and by $x = F^{-1}V_2$ respectively. However, depending on the measurement space and prior, an objective might become more practical. The analysis and in-painting objective require the inverse of the dictionary D^{-1}. It exists for orthogonal transformation like the Haar Wavelet transform, but in general does not exist for over-complete dictionaries. For over-complete dictionaries, the Synthesis objective gets used. There are a few notable exceptions like the Starlet Transform,

which is both an over-complete representation but also has an inverse D^{-1} defined. Similarly, the in-painting method is useful when the prior is defined as a convolution with the image, since it can be represented as a multiplication in the Fourier domain. During this project, no reconstruction algorithm was found which uses the in-painting method.

2.3 Compressed Sensing Reconstruction Algorithms in Astronomy

In Astronomy, Compressed Sensing reconstruction algorithms are an active field of research. There is a diverse list of Algorithms. Three are represented here:

- PURIFY [13]
- Vis-CS [14]
- SASIR [7]

PURIFY uses the analysis objective and SDMM as the optimizer. As the prior, it uses a combination of Dirac basis and Daubechies Wavelets. With the SDMM optimizer PURIFY is a scalable approach which can easily be distributed on computing clusters.

Vis-CS uses the synthesis objective and Coordinate Descent as the optimizer. The prior is a dictionary of Gaussian funtions and was developed for x-ray imaging. The reconstruction reduces the number of parameters and can be used for automated reconstruction.

SASIR uses the synthesis objective and FISTA as the optimizer. The prior is the Starlet Transform. The Starlet Transform uses a multi-resolution representation and with it, the SASIR algorithm was able to reconstruct super-resolved image for the LOFAR interferometer. The Starlet Transform was also implemented in this project and compared to standard CLEAN images in section 3.

2.4 Implementation In CASA

The process of reconstructing an image in CASA is split in two separate cycles: The major and the minor cycle. The major cycle transforms the Visibilities to image space and back using the Fourier Transform. The minor cycle is the deconvolution algorithm, which tries to find the true image from a dirty image and a PSF.

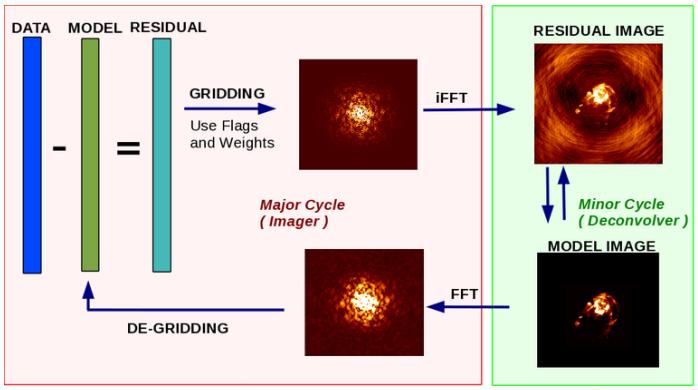

Figure 2: Casa Major Minor Cycle. Source [15]

The first major cycle iteration creates the PSF and the dirty image. Then, several minor cycles deconvolve the dirty image. The major cycle then continues and transforms the deconvolved image back to Visibilities. At this point, the deconvolved Visibilities are called ”model” Visibilities. The major cycle ends by substracting the model from the measured Visibilities, resulting in the residuals. The next major cycle continues by transforming the residual Visibilities. At the end of several major cycles (and with many, many minor cycle iterations) the model column should contain an approximation of the true visibilities while the residuals should contain the noise.

The major cycle is an expensive operation. It is responsible for creating the dirty image and with that, it is also responsible for handling any wide field imaging effects. The major and minor cycle separation is built for CLEAN. A Compressed Sensing deconvolution is able to reconstruct the image in one major cycle iteration.

Future instruments like SKA produce more data and require image reconstruction on a new scale. A big question for reconstruction algorithms is how well do they scale on very large image sizes and how well can they be distributed. The CLEAN algorithm is simple compared to a Compressed Sensing Reconstruction, CLEAN may have the edge in scalability. However, in real world applications CLEAN gets used as a minor cycle deconvolver, and it may need several expensive major cycles to reconstruct an image. The SASIR and PURIFY algorithms include the major cylce operations in the data term. With a distributed optimizer like SDMM, a Compressed Sensing Reconstruction can solve both, major and minor cycle operations and has the potential to scale better on large problem sizes.

3 Reconstruction of Supernova Remnant G55

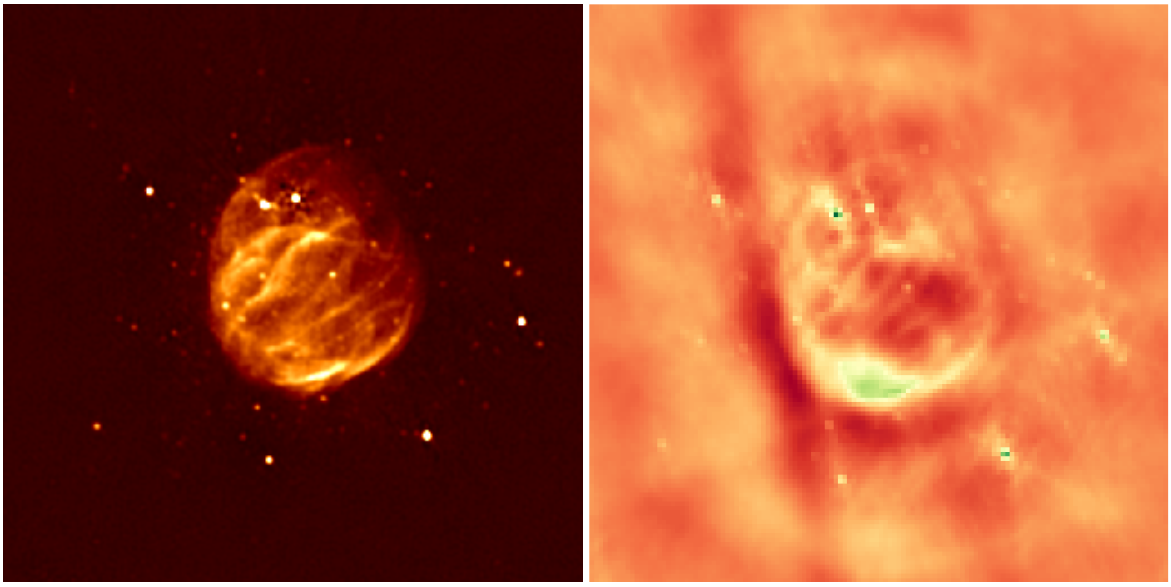

(a) Reconstruction by NRAO. Source:[16] *(b) Dirty Image*

Figure 3: SNR G55 source observed by VLA.

The supernova remnant (SNR) G55 was observed by VLA. 10 seconds of the 8 hour observation is publicly available through the CASA imaging tutorial[17]. 3b is the dirty image calculated from the 10 second observation. The full 8 hours are not readily available. The image 3a is a reconstruction from an unknown VLA observation. The deconvolution algorithm is also unknown. For this project, the image 3a is assumed to show the true image of the sky.

The image 3a shows G55 to be a slightly ”egg shaped” extended emission with six strong point sources. Several fainter point sources are inside and around the egg shaped extended emission. The dirty image 3b shows a corrupted version of G55. The six strong point sources are clearly visible as are the brighter parts of the extended emission. The dirty image also shows a negative ”trench” striking through the image as well as brighter regions around the remnant.

The images in figure 3 spans a size of 55 arc-minutes. For small field of view imaging, images with half the size are usually the limit. In the real world, wide field imaging would be used. In this project, small field of view imaging was used because it is quicker to compute. It limits the dynamic range of the dirty image, the whole task gets harder for the reconstruction algorithm.

The CLEAN algorithm gets compared to Compressed Sensing Reconstructions. The parameters of CLEAN were taken from the CASA imaging tutorial[17]. The reconstructed images of Compressed Sensing are constrained to have no negative pixels. Negative pixels are not physically plausible and was shown to improve Compressed Sensing reconstructions for synthetic data[18]. In total six different priors were tested with the analysis objective:

1. No Regularization
2. L1
3. L2
4. L1+L2
5. Total Variation

6. Starlet Transform

To reduce the memory requirements, the PSF was truncated. Any value smaller than 0.02 of the PSF was truncated to zero. The current implementation requires a quadratic amount of memory per pixel. The images here have a size of $128 * 128$ pixels, which was the maximum for current desktop machines.

The regularization parameter λ needs to be estimated for each prior. The Miller[19] λ estimation was used and is shown in equation (3.1). An approximate solution is needed for the bounds e and E. In this project, the result with no regularization was used for the λ estimation. For practical applications the image effectively gets reconstructed twice. Other Compressed Sensing Reconstructions approximate x of equation (3.1) by running their optimizer a fixed number of iterations without regularization, which reduces the computational costs.

$$\lambda = e/E \qquad \|I_{dirty} - x \star PSF\|_2^2 \leq e \qquad p(x) \leq E \tag{3.1}$$

Two figures compare the Dirty Image, CLEAN and the Compressed Sensing Reconstrutions. Figure 4 shows the reconstructed images on the same intensity scale. Figure 5 shows the flux profile of the reconstructed images.

CLEAN: CLEAN detects the brightest point sources, but finds only part of the extended emission. The top half of the ”egg” emission is missing. The structures of the remnant are blurred compared to the Compressed Sensing reconstructions. With the parameters of the imaging tutorial, CLEAN models the trench as a region with negative emissions. This is not physically plausible, although the behaviour can be changed with additional parameters. The profile 5 shows that CLEAN accurately reconstructs the flux of the large peaks, although the peaks are wide in comparison.

No Regularization: Detects the egg-head of the remnant and the non-negativity constraint keeps it from modelling the negative trench. It detects the smaller point sources around the remnant, but also detects ”fake” extended emissions all around. The profile 5 shows two smaller peaks in the center (30 arc-minutes) which may represent the ”ribs” of the extended emissions in the NRAO reconstruction 3a as do the two small point sources at the edge of the remnant (20 arc-minutes). However, the dirty image has a rise in flux at the borders of the image, which is likely an artefact of the measurement, considering it does not exist in the NRAO reconstruction 3a.

L1: There is almost no visible difference between no regularization and L1. This is possibly an interaction with the Miller λ estimation, since the result of no regularization was used to estimate the λ of L1. The L1 regularization removes part of the ”fake” extended emission, particularly in the top region, but also a few structures in the center. The peaks in the profile 5 of L1 and no regularization are narrower than CLEAN, although they do not reach the same peak flux. L1 is prone to produce unlikely extended emissions: L1 also tries to approximate extended emissions with a number of faint point sources. This can introduce artefacts like pixel wide holes in extended emissions and produces a ”bumpy” profile at the fake extended emissions (at 10 and 50 arc-minutes).

L2: Forces the extended emissions to be more smooth. It also considerably lowers the flux of bright point sources. The profile 5 shows L2 forces the bright peak to widen and lower. The peak is almost as wide as the CLEAN reconstruction. In the remnant center, it blurs structures.

L1+L2: Since L1 does a good job with point sources, but needs to be more continuous for extended emissions, why does one not combine both regularizations? The flexibility of Compressed Sensing Reconstructions allows for it. Sadly, the result is indistinguishable from the L1 regularization. In the dirty image, all pixels are very close to zero (Maximum: 0.0076 in Dirty Image). If the L1 and L2 regularization receive the same λ, the L1 term dominates. If the dirty image would contain pixels much larger than 1, then the L2 term would dominate.

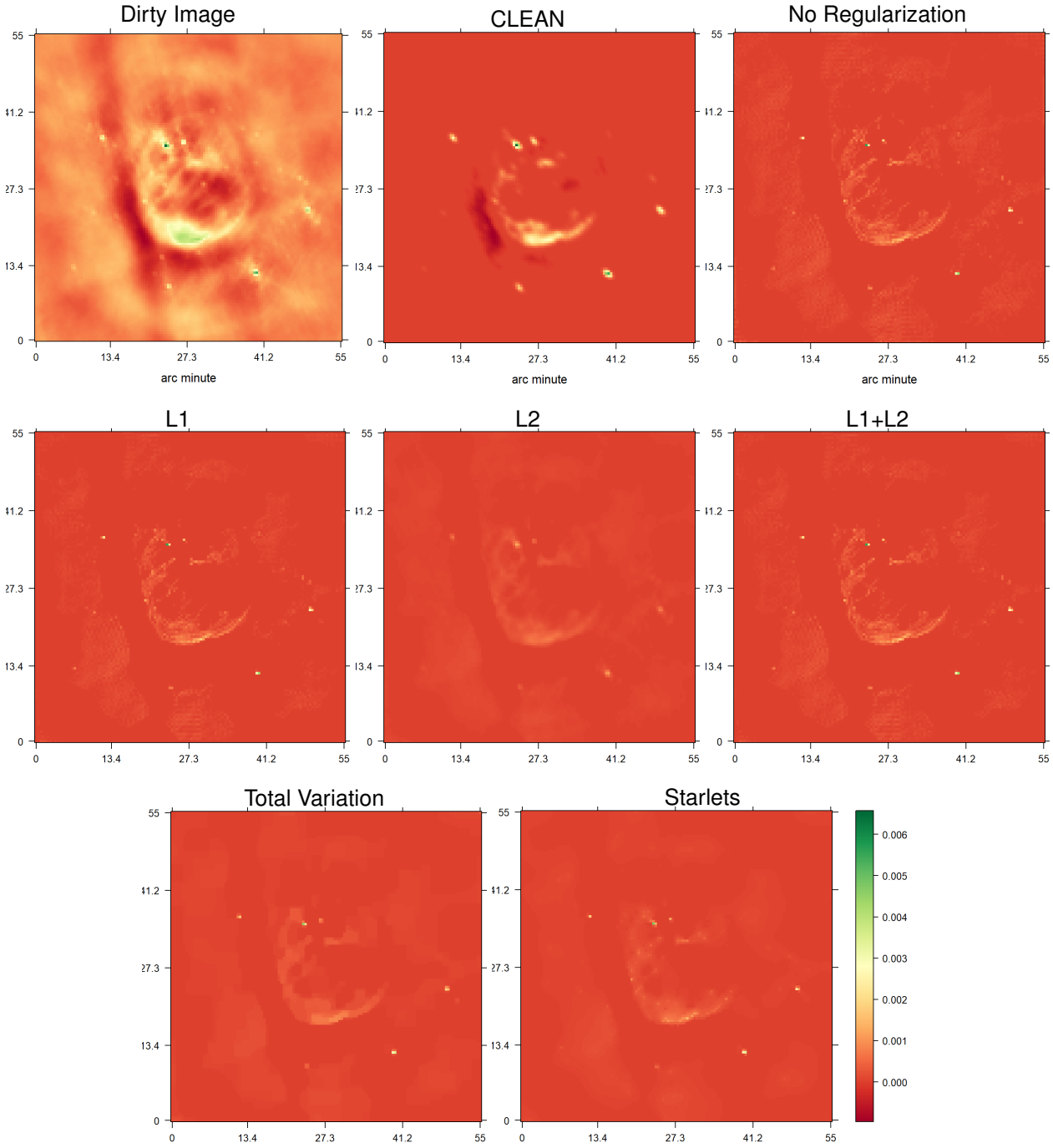

Figure 4: Reconstructed images of CLEAN and the different Compressed Sensing priors.

Total Variation: A simple prior that has its origins in image de-noising. The objective is to reduce the gradients over the image. With an infinite λ, the Total Variation forces all pixels of the reconstruction to have the same value. The idea of the prior is to work well for both extended emissions and point sources. It has trouble with point sources inside extended emissions. In the profile, it is clearly visible how Total Variations cuts the peaks inside the remnant.

Starlets: Is a more sophisticated prior which also tries to model both point sources and extended emissions. It locates the point sources accurately. In the profile 5 it also finds the faint point sources in the extended emission. However, it also smoothed out the structure inside the remnant. For the LOFAR instrument, the starlet regularization was able to find smaller structures than the antenna beam-width[7]. The smallest starlet

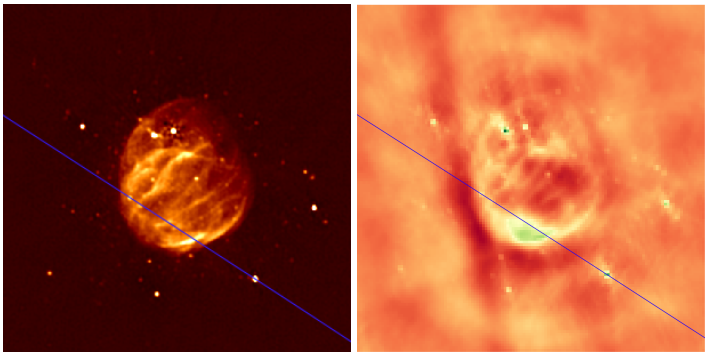

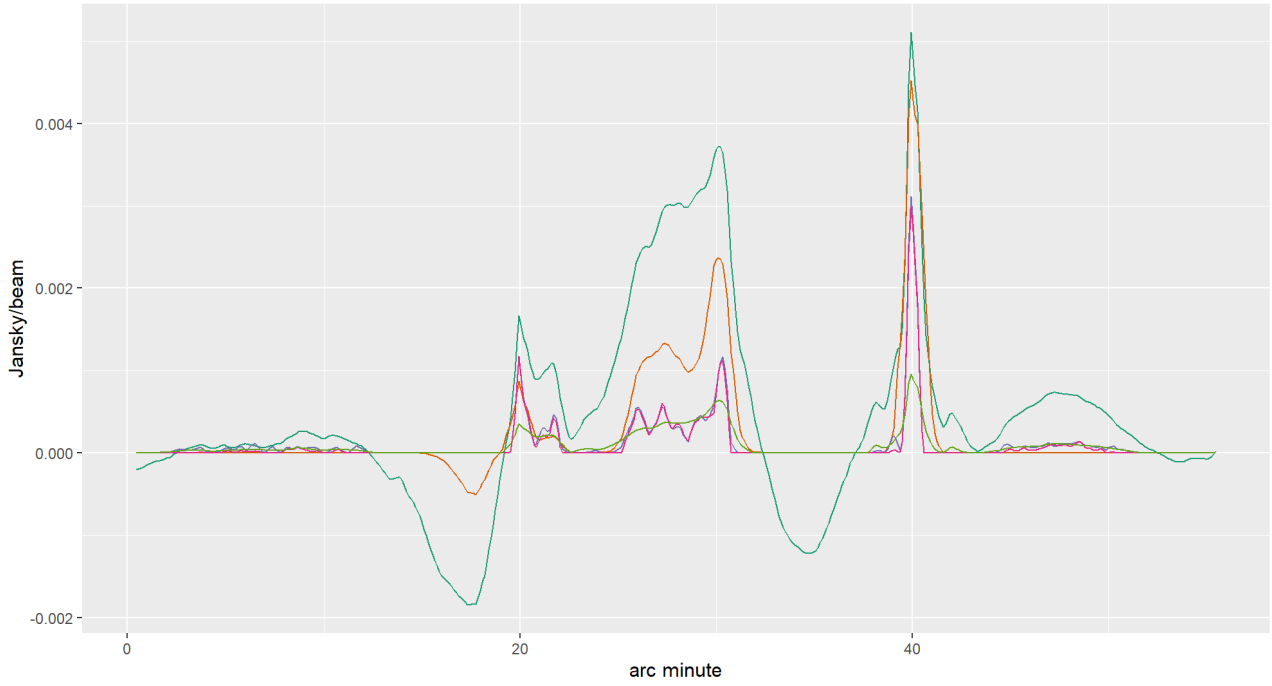

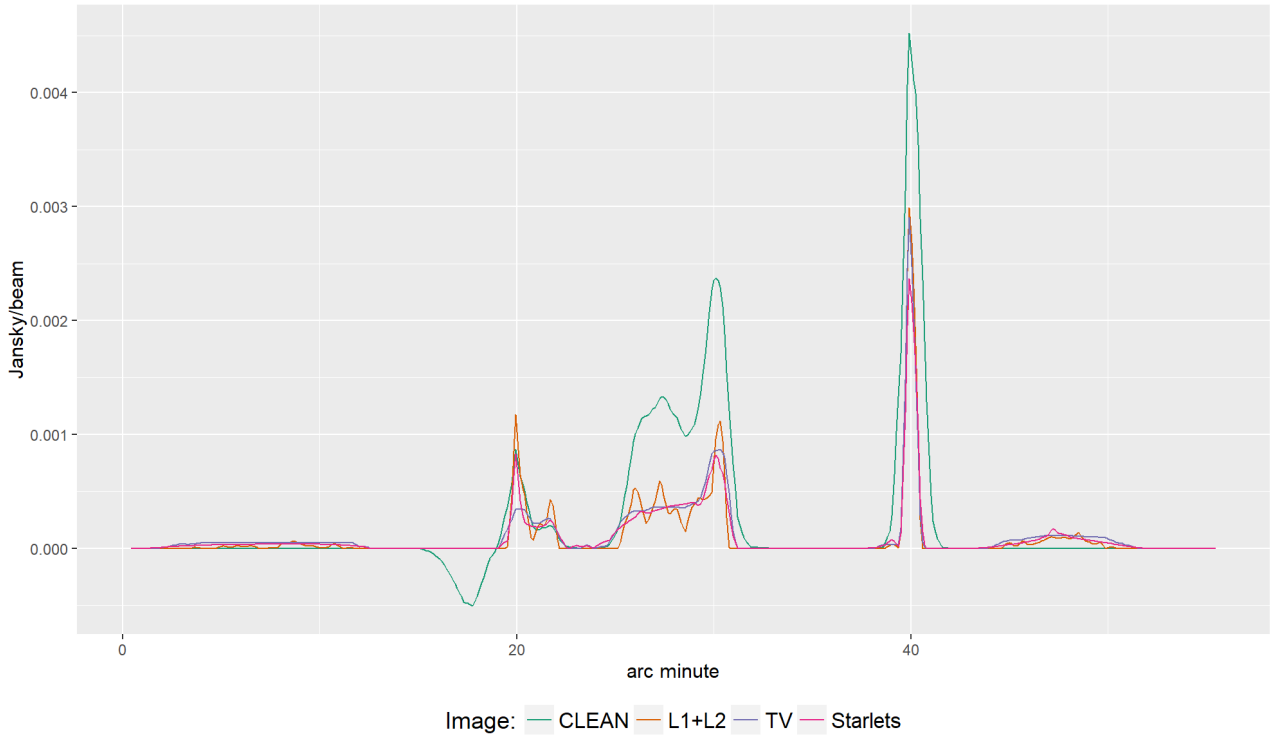

Figure 5: Intensity profile of CLEAN and the different Compressed Sensing Regularizations.

has a $5 * 5$ pixels dimension. For this reconstruction, the antenna beam-width is about two pixels wide. The resolution might be too coarse for the starlet regularization.

CLEAN produces the accurate flux for strong point sources, even though in other reports Total Variation and Starlets reconstructed comparable peak flux to CLEAN [20][18].This is due to the implementation in CASA: The PSF CASA produces does not sum up to one. Convolving an image with the PSF increases the total flux, and naturally a deconvolution decreases the flux. CLEAN is the only algorithm that comes close to the measured flux, because in the last iteration, the reconstructed image gets convolved with the beam pattern (usually a 2d gaussian function), which is also not normalized. If we also convolve the Compressed Sensing reconstructions with the beam pattern (and smear away details), the fluxes become similar.

In this example, the L1 normalization was able to find smaller, plausible structures than CLEAN inside the remnant. Outside the remnant, all Compressed Sensing Reconstructions found ”fake” extended emissions. The L2 and starlet were also expected to find smaller structures. One possible explanation is that the antenna beam-width is about two pixels wide. Any structure smaller than the beam-width is one pixel wide. For higher resolutions it is expected that L1 introduces more artefacts. The current implementation cannot increase the resolution since it needs a quadratic amount of memory per pixel.

4 Future in Compressed Sensing Reconstruction

The flexibility of Compressed Sensing Reconstructions allows us to change the prior according to our knowledge, all while keeping the same objective and optimization algorithm. The prior can be updated as our knowledge increases. The reconstruction was able to find plausible structures smaller than the antenna beam-width. Using Compressed Sensing Reconstructions gives us theoretical guarantees that, if our prior models the observation well enough, we reconstruct the true image from under-sampled measurements.

A proof of Compressed Sensing Reconstruction was implemented in CASA as a minor cycle deconvolver. It takes the dirty image and point spread function as input and calculates the optimal deconvolution according to the objective. The current implementation has a quadratic memory requirement. It does not scale to any practical image size for VLA observations. New interferometers like MeerKAT will require even larger images. The current implementation is not suited for large scale reconstructions.

Self-calibration is a task which was not covered in this project. Self-calibration aims to reconstruct both the image and the the antenna gain calibration from the same measurements. Here with Compressed Sensing Reconstructions one may be able to apply convex optimization techniques to self-calibration, and find the global optimum of both calibration and reconstructed image.

New interferometers are built with wide field of view imaging in mind, which introduces new measurement effects that a reconstruction algorithm should account for. State of the art Compressed Sensing Reconstructions take the measurements as input and also correct wide field of view effects. Due to the CASA interface, the current implementation is restricted to be in the image space, the effects of wide field of view are currently handled by CASA. The next step is a Compressed Sensing Reconstruction which accounts for the effects of wide field imaging and scales to astronomical image sizes.

References

[1] Emmanuel J Candès, Justin Romberg, and Terence Tao. Robust uncertainty principles: Exact signal reconstruction from highly incomplete frequency information. IEEE Transactions on information theory, 52(2):489–509, 2006.

[2] David L Donoho. Compressed sensing. IEEE Transactions on information theory, 52(4):1289–1306, 2006.

[3] JA Högbom. Aperture synthesis with a non-regular distribution of interferometer baselines. Astronomy and Astrophysics Supplement Series, 15:417, 1974.

[4] FR Schwab. Relaxing the isoplanatism assumption in self-calibration; applications to low-frequency radio interferometry. The Astronomical Journal, 89:1076–1081, 1984.

[5] JW Rich, WJG De Blok, TJ Cornwell, Elias Brinks, Fabian Walter, Ioannis Bagetakos, and RC Kennicutt Jr. Multi-scale clean: A comparison of its performance against classical clean on galaxies using things. The Astronomical Journal, 136(6):2897, 2008.

[6] Urvashi Rau and Tim J Cornwell. A multi-scale multi-frequency deconvolution algorithm for synthesis imaging in radio interferometry. Astronomy & Astrophysics, 532:A71, 2011.

[7] Julien N Girard, Hugh Garsden, Jean Luc Starck, Stéphane Corbel, Arnaud Woiselle, Cyril Tasse, John P McKean, and Jérôme Bobin. Sparse representations and convex optimization as tools for lofar radio interferometric imaging. Journal of Instrumentation, 10(08):C08013, 2015.

[8] ams.org. Compressed sensing makes every pixel count, 2007.

[9] Emmanuel J Candes and Yaniv Plan. A probabilistic and ripless theory of compressed sensing. IEEE transactions on information theory, 57(11):7235–7254, 2011.

[10] Jean-Luc Starck, Fionn Murtagh, and Mario Bertero. Starlet transform in astronomical data processing. Handbook of Mathematical Methods in Imaging, pages 2053–2098, 2015.

[11] Jean-Luc Starck, David L Donoho, and Emmanuel J Candès. Astronomical image representation by the curvelet transform. Astronomy & Astrophysics, 398(2):785–800, 2003.

[12] Gurobi Optimization. Gurobi optimizer, 2018.

[13] Rafael E Carrillo, Jason D McEwen, and Yves Wiaux. Purify: a new approach to radio-interferometric imaging. Monthly Notices of the Royal Astronomical Society, 439(4):3591–3604, 2014.

[14] Simon Felix, Roman Bolzern, and Marina Battaglia. A compressed sensing-based image reconstruction algorithm for solar flare x-ray observations. The Astrophysical Journal, 849(1):10, 2017.

[15] National Radio Astronomy Observations. tclean overview, 2016.

[16] National Radio Astronomy Observations. Glowing bubble of an exploded star, 2016.

[17] National Radio Astronomy Observations. Vla casa imaging-casa5.0.0, 2017.

[18] Jason D McEwen and Yves Wiaux. Compressed sensing for radio interferometric imaging: Review and future direction. In Image Processing (ICIP), 2011 18th IEEE International Conference on, pages 1313–1316. IEEE, 2011.

[19] Keith Miller. Least squares methods for ill-posed problems with a prescribed bound. SIAM Journal on Mathematical Analysis, 1(1):52–74, 1970.

[20] Hugh Garsden, JN Girard, Jean-Luc Starck, Stéphane Corbel, C Tasse, A Woiselle, JP McKean, Alexander S Van Amesfoort, J Anderson, IM Avruch, et al. Lofar sparse image reconstruction. Astronomy & astrophysics, 575:A90, 2015.

List of Figures

List of Tables

5 Ehrlichkeitserklärung

Hiermit erkläre ich, dass ich die vorliegende schriftliche Arbeit selbstständig und nur unter Zuhilfenahme der in den Verzeichnissen oder in den Anmerkungen genannten Quellen angefertigt habe. Ich versichere zudem, diese Arbeit nicht bereits anderweitig als Leistungsnachweis verwendet zu haben. Eine Überprüfung der Arbeit auf Plagiate unter Einsatz entsprechender Software darf vorgenommen werden.
Windisch, August 14, 2018

Jonas Schwammberger